

Inclusive cross-sections of (p, xp) and $(p, x\alpha)$ reactions on ^{56}Fe at $E_p = 29.9$ MeV

A. Duisebayev and K. M. Ismailov

Institute of Nuclear Physics, National Nuclear Center, Republic of Kazakhstan

I. Boztosun*

Department of Physics, Erciyes University, Kayseri, Turkey

(Received 25 June 2005; published 16 November 2005)

In this paper, we present new experimental data measured at $E_p = 29.9$ MeV for the inclusive reactions (p, xp) and $(p, x\alpha)$ on nucleus ^{56}Fe . We investigate the adequacy of the theoretical models in explaining the measured experimental data, and we determine the contributions of multistep direct and multistep compound processes in the formation of the cross-sections. We show that the traditional frameworks are valid for the description of the new experimental data, and our measurements agree with previous measurements for the (p, xp) and $(p, x\alpha)$ reactions on the ^{54}Fe nucleus. The only exception is within the energy region of $E_p = 15$ and 25 MeV for both reactions, where the cross-section for the ^{56}Fe nucleus is smaller than the cross-section for the ^{54}Fe nucleus.

DOI: [10.1103/PhysRevC.72.054604](https://doi.org/10.1103/PhysRevC.72.054604)

PACS number(s): 25.40.-h, 24.60.Dr, 24.60.Gv, 24.50.+g

I. INTRODUCTION

Working out the preequilibrium decay mechanism in nuclear reactions, which reflects the dynamics of the formation of the excited system and its evolution to the equilibrium state, remains a problem in nuclear reaction theory. The problem is largely connected with obtaining new experimental data on double-differential cross-sections in (p, xp) , (p, xd) , etc., reactions. It is anticipated that the availability of high-quality experimental data on reactions with different proton energies [1] could address this problem.

The reactions induced by protons within the energy range of 10–2000 MeV play a crucial role in applied research on secure and wasteless nuclear power system creation (accelerator+subcritical reactor). In order to establish such a system, experimental data on key parameters of nucleon interaction, cross-sections of interaction, energy spectra, and angle distributions of secondary particles ($^1,^2,^3\text{H}$, $^3,^4\text{He}$, etc.) need to be obtained. These secondary particles can be agents initiating a reaction with neutron emission. The testing and perfection of the theoretical methods and codes for describing the experimental measurements are also very important.

Therefore, in this paper, the ^{56}Fe nucleus has been chosen as the object of our investigation since it is one of the basic constructional materials of a hybrid nuclear-energy installation. Early experimental studies on the targets of $^{54,56}\text{Fe}$ nuclei [3–9] focused on the emission of protons, deuterons, and α particles. The double-differential cross-section measurements, angle-integrated spectra, and energy-binned angular distributions obtained from these experimental studies have been compared with the predictions of the preequilibrium reaction theory (see a recent review by Koning and Duijvestijn [10] for a detailed discussion). Initial experimental measurements for the reactions (p, xp) and $(p, x\alpha)$ on nuclei of isotope ^{54}Fe at $E_p = 29.0$ and 39.0 MeV have been provided in Ref. [6], and the energy spectra of secondary particles have been analyzed

within the intranuclear cascade and evaporation models. An acceptable description of the experimental data has been achieved only for a spectrum higher than 20.0 MeV.

The Japanese group [11] has investigated the cross-sections of the reaction (p, xp) on $^{54,56}\text{Fe}$ nuclei targets with a thickness of 500 mg/cm² at the energy 26.0 MeV. The experimental data have been analyzed within the framework of Feshbach-Kerman-Koonin (FKK) preequilibrium theory for the preequilibrium processes by using the code FKK-GNASH and within the framework of the Hauser-Feshbach model for compound processes.

It is clear that protons in the energy region of 30 MeV have not been studied in detail. Extending the experiment in this direction allows us to view the mechanisms of the reaction and the level of energy dependence in detail and to use these observations for adequate analysis within the framework of the preequilibrium reaction theory.

Therefore, in our experiment, we considered the (p, xp) ^{56}Fe and $(p, x\alpha)$ ^{56}Fe reactions at $E_p = 29.9$ MeV, within the angle range of 30–135°. In the following section, we present our experimental method, details of the measurement, and experimental results. Section III is devoted to the theoretical analysis of the measured experimental data by the exciton model and quantum mechanical representations. Finally, we present our summary and conclusion in Sec. IV.

II. EXPERIMENT AND RESULTS

The experimental cross-section measurements of reactions (p, xp) and $(p, x\alpha)$ were carried out on a beam of accelerated protons at an energy of 29.9 MeV on the isochronous cyclotron, U-150M, at the Institute of Nuclear Physics, National Nuclear Center, Republic of Kazakhstan, by using a self-supporting target ^{56}Fe . The properties of the target nucleus are given in Table I. The measurements were conducted within the angle range of 30–135°, at intervals of 15°, in the laboratory system.

The registration and identification of the reaction products were carried out by a system of multiprogramming analysis, based on the use of the ΔE - E method, ORTEC, and PC-

*Electronic address: boztosun@erciyes.edu.tr

TABLE I. Characteristics of the target nucleus.

	Thickness (mg/cm ²)	Enrichment (%)
⁵⁶ Fe	2.7	95

spectrometric lines. The block scheme of the registration system is presented in Fig. 1. The detector telescope had a silicon surface-barrier detector ΔE with a thickness of 30 microns and E with a thickness of 2000 microns for the reaction $^{56}\text{Fe}(p, x\alpha)$. For the reaction $^{56}\text{Fe}(p, xp)$, the thickness of the silicon surface-barrier detector ΔE was 500 microns, and the thickness of the stop detector of total absorption-crystal CsI(Tl) was 25 mm. The solid angles of the telescopes were made equal to 2.72×10^{-5} and 2.59×10^{-5} sr, respectively. The energy calibration of the spectrometers was carried out on the kinematics of residual nuclei levels in the $^{12}\text{C}(p, x)$ reaction and protons of recoil. The total energy resolution of the system basically was equated to 400 keV and was determined by the energy resolution of the accelerated proton beams. One should note that the real line spectra might be distorted by the impurity of the light elements in the target nucleus, accidental coincidences, and background. Therefore, at each angle, the spectra were measured both with and without the target, as well as with the spectra of light elements such as ^{12}C and ^{16}O .

Thus, the systematic uncertainties were conditioned by the uncertainties in determining the target thickness ($\sim 7\%$), the calibration of the current integrator ($\sim 1\%$), and the solid angle of the spectrometer ($\sim 1.3\%$). The energy of the accelerated particles was measured accurately within 1.2%. The uncertainties of the registration angle were less than 0.5%. The whole systematic error was less than 10%. The statistical uncertainties at a long exposition time of the double-differential cross-sections were less than 10% for protons and less than 20% for α particles in the high-energy region of the spectra.

The results of the measurements are shown in Fig. 2 for the $^{56}\text{Fe}(p, x\alpha)$ reaction and in Fig. 3 for the $^{56}\text{Fe}(p, xp)$ reaction together with analogical data on an isotope of the iron nucleus ^{54}Fe at 29.0 and 39.0 MeV, presented in Ref. [6]. In accordance with the measurement of Ref. [6], the cross-sections of reactions $^{56}\text{Fe}(p, x\alpha)$ (Fig. 2) and $^{56}\text{Fe}(p, xp)$ (Fig. 3) practically coincide with the cross-sections of the appropriate reactions on ^{54}Fe . The only exception is in the

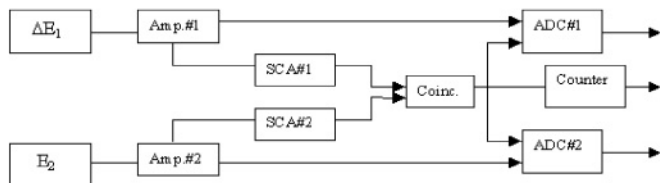


FIG. 1. Block scheme of registration system showing spectroscopic amplifiers (Amp.), single-channel analyzers (SCA), scheme of coincidences (Coinc.), counter scheme (Counter), and analog-digital converters (ADC).

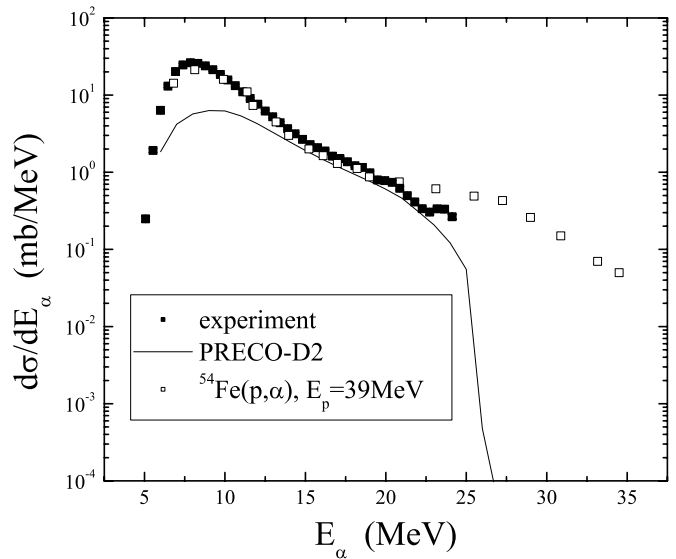


FIG. 2. Integral cross-section of the $^{56}\text{Fe}(p, x\alpha)$ reaction at $E_p = 29.9$ MeV (filled squares). $^{54}\text{Fe}(p, \alpha)$ reaction at $E_p = 39.0$ MeV [6] is also shown to illustrate the isotope dependence of the reactions (empty squares).

energy region $E_p = 15\text{--}25$ MeV for both reactions, where the cross-section for ^{56}Fe is less than the cross-section for the ^{54}Fe nucleus. We obtained the experimental partial cross-section by integrating the integral spectra ($d\sigma/dE$) on energy. The experimental partial cross-sections of reactions $^{56}\text{Fe}(p, x\alpha)$ and $^{56}\text{Fe}(p, xp)$ are given in Table II.

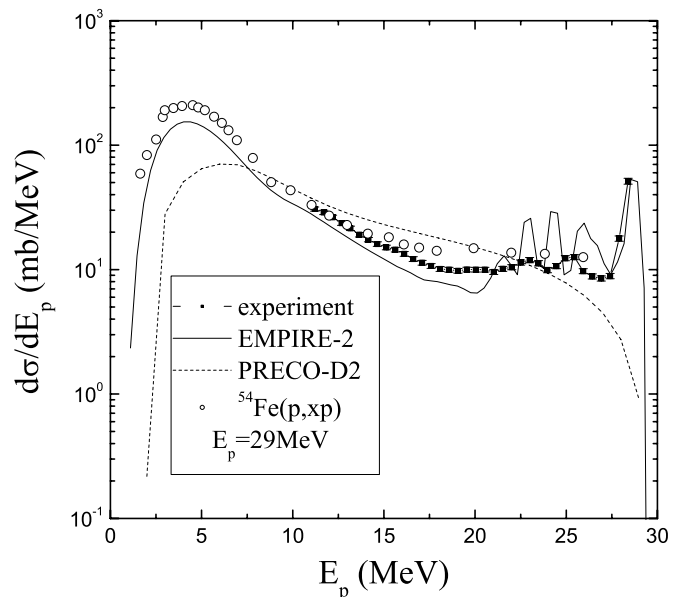


FIG. 3. Integral cross-section of the $^{56}\text{Fe}(p, xp)$ reaction at $E_p = 29.9$ MeV (filled circles). $^{54}\text{Fe}(p, xp)$ reaction at $E_p = 29.0$ MeV [6] is also shown to illustrate the isotope dependence of the reactions (empty circles).

TABLE II. Experimental partial cross-section of the reactions $(p, x\alpha)$ and (p, xp) .

^{56}Fe	Energy range (MeV)	σ (mb)
$(p, x\alpha)$	5–25	132.2 ± 1.2
(p, xp)	11–27	219.41 ± 1.4

III. ANALYSIS OF THE RESULTS

Many different theoretical approaches have been used to describe the preequilibrium reaction data over a wide range of incident energies (see Ref. [10–15] for a detailed discussion). In this paper, the analysis of the experimental results has been conducted in the Griffin exciton model [16] of the preequilibrium decay of nuclei. The program PRECO-D2 [17], which describes the emission of particles with mass numbers from 1 to 4, has been used in our theoretical calculations. The Griffin exciton model is a statistical model, which describes the excited levels of the intermediate system in terms of the single-particle shell model, i.e., characterized by the number of the excited particles (above the Fermi level) and holes (below the Fermi level). It is assumed that the evolution of the system occurs through a sequence turning into complicated configurations and the emission of particles is possible in each phase of this evolution. The conditions of the intermediate system are divided into two classes: bound and unbound. This allows the calculation of the integrated cross-sections on an angle for the statistical multistep direct (MSD) and multistep compound (MSC) processes [18] in the exciton model. The calculated contributions of the MSD and MSC processes in the formation of the total cross-section of reactions $^{56}\text{Fe}(p, xp)$ and $^{56}\text{Fe}(p, x\alpha)$ are shown in Figs. 4 and 5. The contribution of

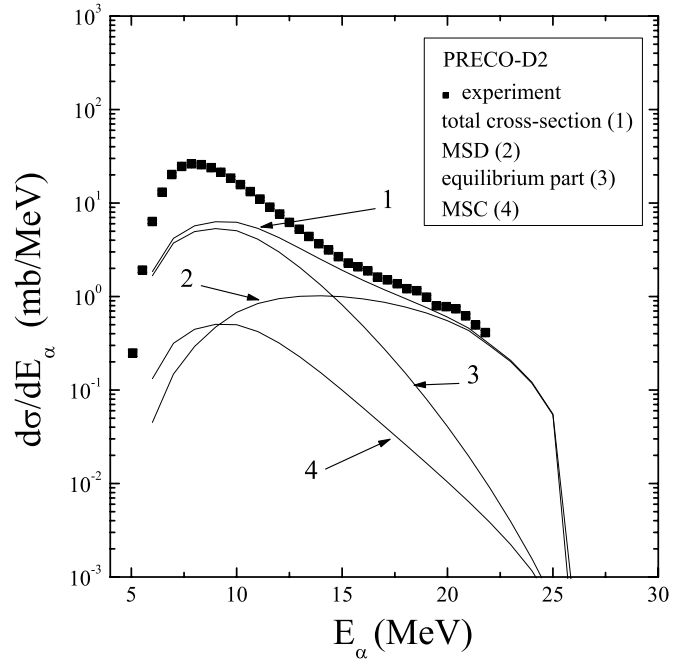


FIG. 4. Contribution MSD and MSC mechanisms to the formation of the integral spectra of reactions $^{56}\text{Fe}(p, x\alpha)$ at $E_p = 29.9$ MeV obtained by using PRECO-D2.

additional MSD components, which are not taken into account by the Griffin model, have been determined semiempirically by taking into account the direct nucleon transfer reaction and knock-out direct processes, including cluster freedom degrees. Evaporation from the equilibrium state of the nucleus has been included in the total cross-section. The configuration $(1p0h)$

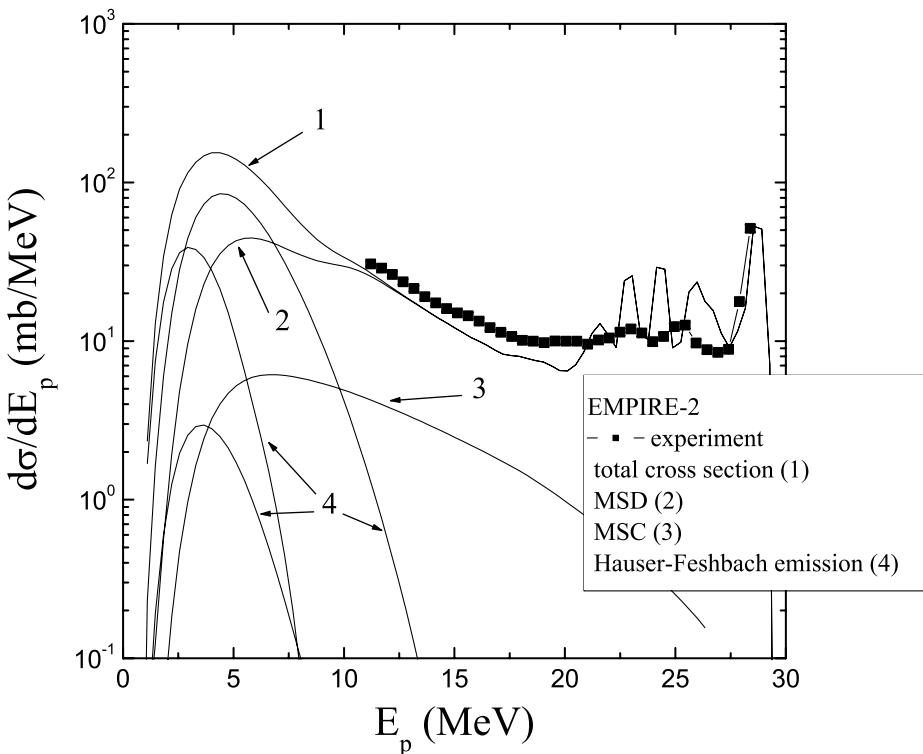


FIG. 5. Same as Fig. 4, but for $^{56}\text{Fe}(p, xp)$ at $E_p = 29.9$ MeV obtained by using EMPIRE-II.

TABLE III. Theoretical contributions of various mechanisms forming the total cross-sections of reactions ($p, x\alpha$) and (p, xp).

	Energy range (MeV)	Total cross-section (mb)	Cross-section contribution (mb)			
			MSD	MSC	Equilibrium	Hauser-Feshbach emission
PRECO-D2 $^{56}\text{Fe} (p, x\alpha)$	6–28	46.8	11.3	3.2	32.24	—
EMPIRE-II $^{56}\text{Fe} (p, xp)$	1–30	1083.6	559.2	64.9	—	459.5

has been accepted as the initial particle-hole configuration in all calculations.

The density of the particle-hole state is given by

$$\omega(p, h, E) = \frac{g(gE - A_{\text{ph}})^{n-1}}{p!h!(n-1)!}, \quad (1)$$

where

$$A_{\text{ph}} = \frac{(p^2 + h^2) + (p - h) - 2h}{4}. \quad (2)$$

The single-particle density of the levels has been accepted as $g = A/13$. The optical potential parameters of Huizenga [19] have been used for α particles, and those of Becchetti and Greenlees [20] for protons.

The comparison of the experimental results and the theoretically calculated spectra are shown in Figs. 4 and 5. These figures show that the basic contribution to the hard part of the total cross-section is caused by the MSD mechanism. It is also observed that the evaporated part of the cross-section is underestimated within the framework of the exciton model used. This may be because the preferred approach gives only the preequilibrium part of the MSC process without taking into account the emission from the complex equilibrium configuration of the compound system. Therefore, the analysis of the experimental cross-sections of the $^{56}\text{Fe}(p, xp)$ reaction is carried out within the Hauser-Feshbach theory by considering the multiparticle emission of both single-charged (protons, deuterons) and two-charged (α particles) fragments by using the program EMPIRE-II [21]. In this code, the contributions of statistical direct and compound processes are described by the optical model (SCAT 2 [22]), multistep direct (ORION+TRISTAN [23,24]), and multistep compound (NVWY [25]) models. The

parameter of the level density has been defined by the Gilbert-Cameron parametrizations [26].

The results of the calculations using the Hauser-Feshbach theory are given in Table III and shown in Figs. 4 and 5. These results indicate that the contribution of the multiparticle compound mechanism determines the emission of protons from 2.5 up to 10 MeV and that the contribution of the multistep direct process ranges from 5 MeV up to the kinematical limit. The form of integral spectra of reaction (p, xp) is determined by the multistep direct processes.

IV. SUMMARY AND CONCLUSIONS

We have presented new experimental data at $E_p = 29.9$ MeV within the angle range of 30–135° for the inclusive reactions (p, xp) and ($p, x\alpha$) on nucleus ^{56}Fe , which has not been investigated in detail so far. We have shown the extension of the preequilibrium reactions to this energy region and have interpreted the results of the experiments. We have also discussed the adequacy of the theoretical models in explaining the measured experimental data. In our theoretical analysis, we have determined the contributions of multistep direct and compound processes in the formation of cross-sections. We assert that the traditional frameworks are valid for the description of the experimental data.

ACKNOWLEDGMENTS

The authors thank Dr. Donna Sue Ozcan and Dr. N. Ayse Odman Boztosun for useful comments and proofreading of the manuscript.

- [1] A. Duisebayev, K. M. Ismailov, and I. Boztosun, Phys. Rev. C **67**, 044608 (2003).
- [2] A. S. Gerasimov and G. V. Kiselev, Physics of Particles and Nuclei (EPAN) **32**, 143 (2001).
- [3] S. M. Grimes, R. C. Haight, K. R. Alvar, H. H. Barschall, and R. R. Borchers, Phys. Rev. C **19**, 2127 (1979).
- [4] A. Marcinkowski, R. W. Finlay, G. Randers-Pehrson, C. E. Briant, R. Kurup, S. Mellema, A. Meigooni, and R. Taylor, Nucl. Phys. **A402**, 220 (1983).
- [5] N. S. Birjukov, B. V. Zhuravlev, A. P. Rudenko, O. A. Salnikov, and V. I. Trykova, Yad. Fiz. **31**, 561 (1980).
- [6] F. E. Bertrand and R. W. Peelle, Phys. Rev. C **8**, 1045 (1973).

- [7] W. Scobel, M. Blann, T. T. Komoto, M. Trabandt, S. M. Grimes, L. F. Hansen, C. Wong, and B. A. Pohl, Phys. Rev. C **30**, 1480 (1984).
- [8] A. Sprinzak, A. J. Kennedy, J. C. Pacer, J. Wiley, and N. T. Porile, Nucl. Phys. **A203**, 280 (1973).
- [9] Y. Watanabe, S. Yoshioka, M. Harada, K. Sato, Y. Nakao, H. Ijiri, S. Chiba, T. Fukahori, S. Meigo, O. Iwamoto, and N. Koori, *in Proceedings of the International Conference on Nuclear Data for Science and Technology*, edited by G. Reffo (Italian Physical Society, Bologna, 1997), p. 580.
- [10] A. J. Koning and M. C. Duijvestijn, Nucl. Phys. **A744**, 15 (2004).

- [11] Y. Watanabe, S. Yoshioka, M. Harada *et al.*, JAERI-Rev. 1997, 97-010 (unpublished), pp. 55-56.
- [12] H. Feshbach, A. Kerman, and S. Koonin, *Ann. Phys. (NY)* **125**, 429 (1980).
- [13] E. Gadioli and P. E. Hodgson, *Pre-Equilibrium Nuclear Reactions* (Oxford University Press, Oxford, 1992).
- [14] R. Bonetti, M. B. Chadwick, P. E. Hodgson, B. V. Carlson, and M. S. Hussein, *Phys. Rep.* **202**, 171 (1991).
- [15] R. Bonetti, A. J. Koning, J. M. Akkermans, and P. E. Hodgson, *Phys. Rep.* **247**, 1 (1994).
- [16] J. J. Griffin, *Phys. Rev. Lett.* **17**, 478 (1966).
- [17] C. Kalbach, PRECO-D2: Program for Calculating Pre-equilibrium and Direct Reaction Double Differential Cross-Sections, LA-10248-MS, February 1985 (unpublished).
- [18] C. Kalbach, *Phys. Rev. C* **23**, 124 (1981); **24** 819 (1981).
- [19] J. R. Huizenga and G. Igo, *Nucl. Phys.* **29**, 462 (1962).
- [20] F. D. Becchetti and G. W. Greenlees, *Phys. Rev.* **182**, 1190 (1969).
- [21] M. Herman, G. Reffo, and H. A. Weidenmüller, *Nucl. Phys.* **A536**, 124 (1992); EMPIRE v2.13 (private communication).
- [22] O. Bersillon, SCAT2: Un programme de modèle optique sphérique, Report CEA-N-2227, NEANDC(FR), INDC(E) 49/L, Oct. 1981 (unpublished).
- [23] T. Tamura, T. Udagawa, and H. Lenske, *Phys. Rev. C* **26**, 379 (1982).
- [24] H. Lenske and H. H. Wolter (private communication to M. Herman).
- [25] H. Nishioka, J. J. Verbaarschot, H. A. Weidenmüller, and S. Yoshida, *Ann. Phys. (NY)* **172**, 67 (1986).
- [26] A. Gilbert and A. G. W. Cameron, *Can. J. Phys.* **43**, 1446 (1965).